



## Vascularized subcutaneous human liver tissue from engineered hepatocyte/fibroblast sheets in mice



Yusuke Sakai <sup>a,\*</sup>, Kosho Yamanouchi <sup>a</sup>, Kazuo Ohashi <sup>b,1</sup>, Makiko Koike <sup>a</sup>, Rie Utoh <sup>b</sup>, Hideko Hasegawa <sup>a</sup>, Izumi Muraoka <sup>a</sup>, Takashi Suematsu <sup>c</sup>, Akihiko Soyama <sup>a</sup>, Masaaki Hidaka <sup>a</sup>, Mitsuhsa Takatsuki <sup>a</sup>, Tamotsu Kuroki <sup>a</sup>, Susumu Eguchi <sup>a</sup>

<sup>a</sup> Department of Surgery, Nagasaki University Graduate School of Biomedical Sciences, 1-7-1 Sakamoto, Nagasaki 852-8501, Japan

<sup>b</sup> Institute of Advanced Biomedical Engineering and Science, Tokyo Women's Medical University, 8-1 Kawada-cho, Shinjuku-ku, Tokyo 162-8666, Japan

<sup>c</sup> Central Electron Microscope Laboratory, Nagasaki University School of Medicine, 1-12-4 Sakamoto, Nagasaki 852-8523, Japan

### ARTICLE INFO

#### Article history:

Received 16 March 2015

Received in revised form

25 June 2015

Accepted 26 June 2015

Available online 27 June 2015

#### Keywords:

Hepatocyte transplantation

Human primary hepatocyte

Fibroblast

Cell sheet

Vascularization

Tissue engineering

### ABSTRACT

Subcutaneous liver tissue engineering is an attractive and minimally invasive approach used to curative treat hepatic failure and inherited liver diseases. However, graft failure occurs frequently due to insufficient infiltration of blood vessels (neoangiogenesis), while the maintenance of hepatocyte phenotype and function requires *in vivo* development of the complex cellular organization of the hepatic lobule. Here we describe a subcutaneous human liver construction allowing for rapidly vascularized grafts by transplanting engineered cellular sheets consisting of human primary hepatocytes adhered onto a fibroblast layer. The engineered hepatocyte/fibroblast sheets (EHFSs) showed superior expression levels of vascularization-associated growth factors (vascular endothelial growth factor, transforming growth factor beta 1, and hepatocyte growth factor) *in vitro*. EHFSs developed into vascularized subcutaneous human liver tissues contained glycogen stores, synthesized coagulation factor IX, and showed significantly higher synthesis rates of liver-specific proteins (albumin and alpha 1 anti-trypsin) *in vivo* than tissues from hepatocyte-only sheets. The present study describes a new approach for vascularized human liver organogenesis under mouse skin. This approach could prove valuable for establishing novel cell therapies for liver diseases.

© 2015 Elsevier Ltd. All rights reserved.

### 1. Introduction

Construction of functional organs with capillary networks *in vitro* and *in vivo* is an attractive for the ultimate goal of regenerative medicine [1–6]. The transplantable liver tissue construction is clearly essential to establish systems to treat liver disease using tissue engineering. However, the reconstruction of liver structures and maintenance of their functions *in vitro* and *in vivo* are

extremely difficult because the liver tissue contains complex liver-specific structures and displays a wide variety of functions [7].

To overcome the problem that liver-specific functions of cultured hepatocytes decrease quickly, many researchers have reported that long-term maintenance of liver-specific functions was achieved using co-culture and/or 3D culture [8–12]. In addition, the reconstruction of liver sinusoids *in vitro* has been achieved by tri-culture of hepatocytes, hepatic stellate cells, and endothelial cells (ECs) on a microporous polyethylene terephthalate membrane [13]. However, the size of the reconstructed liver tissue has usually been limited because hepatocytes consume oxygen at a particularly high rate [14,15]. Several researchers have demonstrated vascular fabrication in cultured tissue using co-culturing with ECs [3], printed rigid 3D filament networks of carbohydrate glass [4], and decellularized liver matrix [16]. However, it has been difficult to construct a functional vascularized liver tissue *in vitro*.

\* Corresponding author.

E-mail addresses: [y.sakai.bioeng@gmail.com](mailto:y.sakai.bioeng@gmail.com) (Y. Sakai), [sueguchi@nagasaki-u.ac.jp](mailto:sueguchi@nagasaki-u.ac.jp) (S. Eguchi).

<sup>1</sup> Present affiliation is Laboratory of Drug Development and Science, Graduate School of Pharmaceutical Sciences, Osaka University, 1–6 Yamada-oka, Suita, Osaka 565–0871, Japan.

The construction of the liver tissue *in vivo* also presents the need for a vascular bed and neovascularization into the transplanted tissue to ensure efficient engraftment and maintenance of proper function. Toward this goal, three-dimensional cell aggregates are usually transplanted into the omental pouch or subrenal capsule, where local blood vessels with high angiogenic potential facilitate tissue survival [2,5,17–19]. In addition, recellularized liver graft using decellularized technology were transplantable organs [16]. However, there are several issues in these transplantation sites such as risks associated with the type of surgery involved in blood vessels.

Vascularized tissue construction under the skin is widely regarded as potentially the safest, quickest, least invasive grafting strategy, retransplantation, and easy removal of transplanted tissues in case of graft failure or tumorigenic transformation [18,20–22], but it has yet to be achieved, because graft failure occurs frequently due to insufficient infiltration of blood vessels [2,5,17,23]. To overcome the issue, previous papers have showed remarkable approaches using cell sheet engineering and neovascularized method. Repeated transplantation of mouse primary hepatocyte sheets has been performed after per-transplant vascularization under skin by implanting a device for the continuous release of angiogenic growth factors [24]. Others showed reconstructed tissue with capillary networks *in vitro* connected with local blood vessels by surgical methods [3,16]. However, these methods have limitations of promptness of treatment such as acute liver disease because it takes at least several days to prepare transplantable tissue from hepatocytes and to prepare the vascular bed.

In this study, we demonstrate a simple and rapid method for producing vascularized subcutaneous human liver tissue (VSLT) *in vivo* by transplantation of engineered hepatocyte/fibroblast sheets (EHFSs) without addition of stem cells or ECs. We show the maintenance of liver-specific functions and reconstructed structures.

## 2. Materials and methods

### 2.1. Human primary hepatocyte isolation

Ethical approval was obtained from the Human Ethics Review Committee of Nagasaki University School of Medicine for human hepatocyte isolation, storage, culture, and transplantation into mice, and informed consent was obtained from all human hepatocyte donors. Resected human liver tissues (approximately 30 g) were obtained during liver surgery (Table 1). Human primary hepatocytes were isolated from human liver tissues by perfusing collagenase (130 U/mL, Wako Pure Chemical, Osaka, Japan) [25,26]. The cell suspension in 25% Percoll Plus solution (GE Healthcare,

Tokyo) was centrifuged at  $70 \times g$  for 7 min at 4 °C to further purify hepatocytes and enrich viable cells. Cell viability was determined by the trypan blue exclusion test, and suspensions with >80% viable cells were used for culture and construction of sheets. The medium for isolation was Dulbecco's modified Eagle's medium (Wako Pure Chemical) supplemented with 10% fetal bovine serum (FBS), 10 mM 4-(2-hydroxyethyl)-1-piperazine ethanesulfonic acid, 2 mM L-glutamine, 100 U/mL penicillin, and 100 µg/mL streptomycin (all from Invitrogen, Carlsbad, CA).

### 2.2. Human fibroblast culture

Normal human diploid fibroblast TIG-118 cells, which derived from human skin (female, 12 years old), were purchased from Health Science Research Resources (JCRB0535; Osaka, Japan) and cultured as a continuous monolayer in 90-mm tissue culture dishes (Nalgene Nunc International, Rochester, NY, USA) containing 10 mL Minimum Essential Medium (Invitrogen) supplemented with 10% FBS, 2 mM L-glutamine, 100 U/mL penicillin, and 100 µg/mL streptomycin. The TIG-118 cells at 90% confluence were treated with 0.25% trypsin-EDTA (Invitrogen), and the cell suspension was obtained.

### 2.3. Human hepatocyte sheet construction

Two types of human primary hepatocyte sheets were constructed using temperature-responsive culture dishes (TRCDs) (UpCell; CellSeed, Tokyo) in accordance with our previous report [27]. To construct EHFSs, human primary hepatocytes obtained as described were plated at  $1.04 \times 10^5$  cells/cm<sup>2</sup> ( $1.0 \times 10^6$  cells/dish) onto a confluent layer of TIG-118 cells plated 3 days previously at  $2.29 \times 10^4$  cells/cm<sup>2</sup> ( $2.2 \times 10^5$  cells/dish) onto non-coated TRCDs (Fig. 1A). To construct hepatocyte-only sheets (HSs), hepatocytes were inoculated onto TRCDs coated with FBS. All the human primary hepatocytes were cultured in Supplemented ISOM's Media (BD Biosciences, San Jose, CA) supplemented with 10% FBS, 100 U/mL penicillin, and 100 µg/mL streptomycin until 24 h after inoculation. The Supplemented ISOM's Media was replaced with 2 mL of Hepato-STIM Culture Medium (BD Biosciences) supplemented with 10% FBS, 2 mM L-glutamine, 100 U/mL penicillin, and 100 µg/mL streptomycin. This medium was changed 1 and 3 days after inoculation. All cells were cultured under a humidified atmosphere of 5% CO<sub>2</sub> and 95% air at 37 °C. After 4 days of hepatocyte culture or coculture, plates were incubated at 20 °C to induce the formation of detached cell sheets. Fibroblast-only sheets (FSs) were also constructed by following the same process. Samples of media were collected after 1–3 days of culture and stored at –20 °C until assayed for human growth factors involved in angiogenesis.

### 2.4. Hepatocyte sheet transplantation under mouse skin

Ethical approval for hepatocyte sheet transplantation was obtained from the Animal Care and Use Committee and the Recombinant DNA Experiment Safety Committee of Nagasaki University and performed according to all protocols approved by the Regulations. The abdominal subcutaneous space for transplantation was created by a tear between the cutaneous and skeletal muscle layer in NOD SCID mice (NOD.CB17-Prkdc<sup>scid</sup>/J; Charles River Japan Inc., Kanagawa, Japan) and in NOG mice (NOD.Cg-Prkdc<sup>scid</sup> Il2rg<sup>tm1Sug</sup>/Jic; Central Institute for Experimental Animals, Kanagawa, Japan) (males, 6–17 weeks old, weighing 20–35 g) (Fig. 1B). The hepatocyte-containing sheets (EHFSs or HSs) after 4 days of culture were subcutaneously-transplanted using a support membrane or a glass plate to facilitate handling, and the supporters were removed at several miniatures after contact of cell sheet into subcutaneous

**Table 1**  
Human liver tissue resource for primary hepatocyte isolation.

	Age	Sex	Disease	Viability [%]
1	70's	M	Hepatocellular carcinoma	93.1
2	70's	M	Intrahepatic cholangiocarcinoma	95.1
3	70's	M	Hepatocellular carcinoma	93.2
4	60's	M	Hepatocellular carcinoma	91.8
5	60's	F	Hepatocellular carcinoma	83.3
6	80's	M	Intrahepatic cholangiocarcinoma	89.7
7	70's	M	Intrahepatic cholangiocarcinoma	93.1
8	60's	F	Cholangiocarcinoma	85.8
9	70's	M	Hepatocellular carcinoma	92.4
10	60's	M	Metastatic liver tumor	95.4
11	70's	F	Intrahepatic cholangiocarcinoma	85.1
12	70's	F	Intrahepatic bile duct cystadenocarcinoma	93.1
13	60's	M	Hilar cholangiocarcinoma	89.8

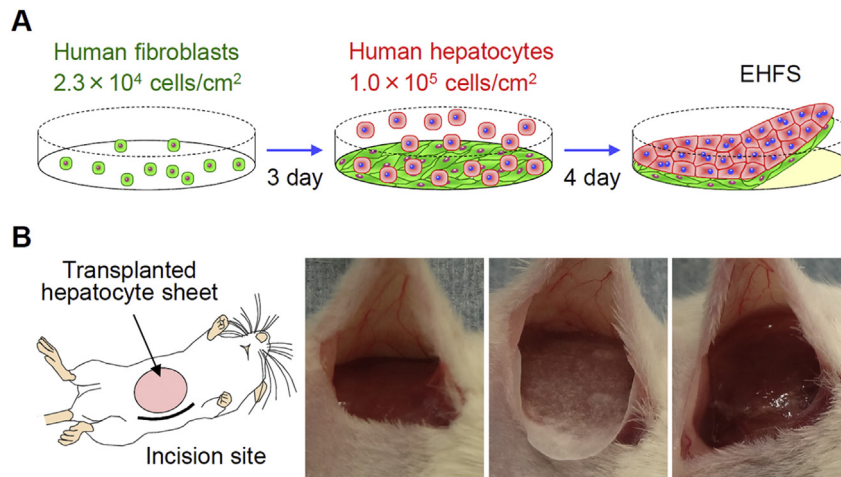


**Fig. 1.** Construction and transplantation of EHFSS. (A) Schematic of EHFSS construction. (B) The processes of hepatocyte sheet transplantation under mouse skin.

site. One cell sheet ( $1.0 \times 10^6$  hepatocytes) was transplanted into each mouse. To demonstrate the advantages of EHFSS, a suspension consisting of hepatocytes ( $1.0 \times 10^6$  cells) and fibroblasts ( $1.5 \times 10^6$  cells) was injected under a mouse's skin. At 1, 2, and 4 weeks after transplantation, 100–200  $\mu$ L of blood was collected from the tail of NOD SCID mice, and the serum samples were stored at  $-20^\circ\text{C}$  until assayed for the concentration of liver-specific human proteins.

### 2.5. Histology

Cell sheets and VSLTs in NOD SCID mice were fixed with 4% paraformaldehyde phosphate buffer solution (Wako Pure Chemical) for 24 h–72 h. Fixed samples were embedded in paraffin, cut into 5- $\mu$ m cross-sections, mounted on MAS-coated slides (Matsunami Glass, Osaka, Japan), and deparaffinized for standard histological staining with hematoxylin and eosin (HE), orange G, azocarmine G, and aniline blue (Azan), or periodic acid-Schiff (PAS) (all from Muto Pure Chemicals, Tokyo). For immunostaining, sections were heated in 10 mM Tris-HCl buffer (pH 9.0) containing 1 mM EDTA using a microwave or autoclave for antigen retrieval, incubated in 3% hydrogen peroxide solution for 10 min to quench endogenous peroxidase activity or Biotin-Blocking System (Dako Japan, Kyoto), and then blocked in Tris-buffered saline (TBS) containing 5% bovine serum albumin (BSA) and 0.1% Tween 20 for 1 h at room temperature. Blocked sections were incubated overnight at  $4^\circ\text{C}$  in TBS +5% BSA, 0.1% Tween 20, and the following antibodies: rabbit anti-human albumin (hALB) (ab2406; 1:3000), mouse anti-human alpha 1-antitrypsin (hA1AT) (ab9399; 1:1500), sheep anti-human blood coagulation factor IX (hF9) (ab128048; 1:100), mouse anti-cytokeratin 18 (CK18) (ab668; 1:500), mouse anti-human vimentin (hVim) (ab8069; 1:500), rabbit anti-cluster of differentiation 31 (CD31) (ab28364; 1:50), rabbit anti-human CD31 (hCD31) (ab76533; 1:250), rabbit anti-Ki67 (ab16667; 1:100) (all from Abcam, Cambridge, MA), or rabbit anti-E-cadherin (E-cad) (sc-7870; 1:100) (Santa Cruz Biotechnology, Santa Cruz, CA). Sections were then incubated for 1 h at room temperature in an appropriate secondary antibody: horseradish peroxidase (HRP)-conjugated goat anti-rabbit IgG (A0545; 1:300), biotin-conjugated goat anti-rabbit IgG (B8895; 1:800), fluorescein isothiocyanate (FITC)-conjugated goat anti-rabbit IgG (F9887; 1:320), FITC-conjugated rabbit anti-mouse IgG (F9137; 1:200), tetramethylrhodamine isothiocyanate (TRITC)-conjugated rabbit anti-mouse IgG (T2402; 1:400), FITC-conjugated ExtrAvidin (E2761; 1:80), TRITC-conjugated ExtrAvidin (E3011; 1:150) (all from Sigma-Aldrich Japan, Tokyo),

or biotin-conjugated donkey anti-sheep IgG (ab97123; 1:500) (Abcam). HRP-conjugated secondary binding was visualized using the Dako liquid DAB + substrate chromogen system (Dako Japan). Nuclei stained with hematoxylin or 4',6-diamidino-2-phenylindole (DAPI; DOJINDO, Kumamoto, Japan). Slides stained with HRP-conjugated secondary antibodies were mounted with PermMount (Fisher Scientific, Atlanta, GA) and slides stained with fluorophore-conjugated secondary antibodies with ProLong gold antifade mounting medium (Invitrogen). Bright-field and fluorescence images were captured using an optical microscope (BX53; Olympus, Tokyo) and a confocal laser scanning microscope (FV10i; Olympus), respectively.

### 2.6. Sheet size and thickness measurements

The exterior photographs of cell sheets were captured to evaluate the cell sheet sizes [27]. The sizes of cell sheets were calculated as the ratio of the cell sheet area to the original TRCD culture surface area. To evaluate the thicknesses of the cell sheets, the HE stained cross-sectional images of the cell sheets were captured. These areas and thickness were measured using the NIS-Elements software program (Nikon, Tokyo).

### 2.7. Ultrastructural analysis (TEM)

EHFSSs and VSLTs in NOG mice at 2 weeks after transplantation were fixed with 2.5% glutaraldehyde in 0.1 M phosphate buffer (pH 7.4), post-fixed in phosphate-buffered 1% osmium tetroxide for 2 h at  $4^\circ\text{C}$ , and then dehydrated through a graded ethanol series. The dehydrated samples were embedded in Epon 812 (TAAB Laboratories Equipment Ltd., Berkshire, England). Ultrathin sections were cut with a diamond knife on an ultramicrotome (Ultracut S, Leica, Austria), double-stained with uranyl acetate and lead nitrate, then imaged under an electron microscope (JEM-1200EX, JEOL, Tokyo) at an accelerating voltage of 60–80 kV.

### 2.8. Human growth factors and liver-specific functions assay (ELISA)

Human platelet-derived growth factor BB (PDGF-BB), vascular endothelial growth factor (VEGF), transforming growth factor beta 1 (TGF- $\beta$ 1), basic fibroblast growth factor (bFGF), hepatocyte growth factor (HGF), and epidermal growth factor (EGF) in culture media samples were measured by using DuoSet ELISA

Development Systems (R&D Systems, Minneapolis, MN) according to the manufacturer's instructions. Human ALB and A1AT in serum samples of NOD SCID mice were measured using rabbit anti-human albumin (6 µg/mL), HRP-conjugated goat anti-human albumin (10 µg/mL) (MP Biomedicals, LLC-Cappel products, Irvine, CA), goat anti-human A1AT (5 µg/mL; Bethyl Laboratories, Montgomery, TX), or HRP-conjugated goat anti-human A1AT (7 µg/mL; Fitzgerald Industries International, Inc., Concord, MA).

### 2.9. Statistical analysis

Data are presented as mean ± standard deviation (SD) from at least 6 time points. Means of continuous numerical variables were compared by Welch's *t*-test, one-way analysis of variance (ANOVA) (Tukey's multiple comparison test), or two-way ANOVA (Sidak's multiple comparison test) (GraphPad Prism version 6.00 for Windows; GraphPad Software, San Diego, CA). Values of \*\**P* < 0.01 and \**P* < 0.05 were considered statistically significant.

## 3. Results

### 3.1. Characteristic morphologies of the EHFS

Human primary adult hepatocytes attached onto the TIG-118 cell layer within 1 h, and these adherent hepatocytes eventually assumed the typical cuboidal shape of mature hepatocytes (Fig. 2A). In contrast, primary hepatocytes cultured alone on a FBS-coated TRCD surface required approximately 4 h to adhere. It normally takes at least 4 days for cultured hepatocytes alone to become fully confluent. EHFSs and HSs were harvested by reducing the culture temperature from 37 °C to 20 °C for approximately 1–2 h (for EHFSs) or 4–12 h (for HSs) on day 4 (Fig. 2B). The reduced temperature initiated the natural detachment of the cells from the edge of the TRCD surface, resulting in floating cell sheets in the culture medium that shrank to approximately 20% of the original culture surface area (Fig. 2B, C). The area of EHFSs were slightly-larger than those of HSs.

Histological cross-sections of both types of hepatocyte sheet showed ubiquitous hepatocyte survival as revealed by HE staining, as well as hepatocytic expression of both hALB and the hepatocyte marker CK18 (Fig. 2D). In EHFSs, almost all hVim-positive fibroblasts (particularly those displaying mesenchymal cell cytoskeleton markers) had migrated from the bottom to the top of the sheet during the 4 days in co-culture with hepatocytes. The cells present in HSs were hVim-negative. The endothelial cell marker hCD31 was expressed only at very low levels in EHFSs and HSs. These EHFSs were approximately 1.6-times thicker than HSs (Fig. 2E). Hepatocytes in EHFSs reconstructed bile canals (BCs), tight junctions (TJs), desmosomes (Ds), and gap junctions (GJs), and adhered to fibroblasts as revealed by TEM (Fig. 2F).

### 3.2. Angiogenic growth factor syntheses *in vitro*

To indicate the possibility of using a one-step subcutaneous hepatocyte transplantation procedure without a pre-transplant vascularization step, synthesis rates of vascularization-associated growth factors *in vitro* were assayed. EHFSs exhibited significantly higher synthesis rates of the angiogenic factors VEGF, TGF-β1, and HGF than the HSs from 1 to 3 days in culture (Fig. 3B, C, E). The synthesis of TGF-β1 and HGF from fibroblasts were upregulated and down-regulated, respectively, by co-culture with hepatocytes. In contrast, PDGF-BB, bFGF, and EGF were not detected in either type of cell sheet (Fig. 3A, D, F).

### 3.3. VSLT construction process from EHFS

Time-dependent VSLTs were investigated by staining with HE, two types of CD31 (non-specific species and human origin), and cell proliferation marker Ki67. The transplanted EHFSs were initially laminated and necrosis occurred at a part of hepatocytes on 1 day after transplantation (Fig. 4A). Although hepatocytes at the outer end of VSLTs were hypertrophic at 7 days, cells were rarely observed at 14 days after transplantation. ECs (CD31-positive) were observed 7 days after transplantation, and many neovascular vessels (Ki67-positive ECs) grew into the liver tissue until 14 days (Fig. 4A–C). In contrast, little expression of Ki67 in hepatocytes was revealed (Fig. 4A). The transplanted EHFSs formed grossly-visible VSLT, which had numerous blood vessels at the edge by day 7 after transplantation (Fig. 4D). The VSLTs indicated an increased red color by day 14 after transplantation (Fig. 4E).

### 3.4. Liver-specific structures of the VSLT

Indeed, VSLT of 100–300 µm thickness at 2 weeks after transplantation contained hepatocytes surrounded by collagen fibers as confirmed by HE and Azan staining, respectively (Fig. 5A). Moreover, VSLT had liver-specific features such as glycogen stores and hALB, hA1AT, and hF9 syntheses as revealed by PAS staining and immunostaining, respectively (Fig. 5A, B). The aggregated hepatocytes formed several linear structures surrounded by human fibroblasts (hVim-positive) and abundant blood vessels (hCD31-positive) and adherens junctions (E-cad) between hepatocytes (CK18-positive). TEM images of VSLTs showed that hepatocytes are adjacent to microvessels supported by fibroblasts through the microvilli (MVs) (Fig. 5C). The VSLTs constructed the ultrastructural features of mature liver, such as BCs and several types of cell adhesions (TJs and Ds). In contrast, transplanted HSs formed simple hepatocyte monolayers that covered only a small area of the transplant site (Fig. 5A).

### 3.5. Liver-specific functions of the VSLT *in vivo*

The *in vivo* liver-specific functionality of transplanted EHFSs is underscored by the concentrations of human proteins detected in the sera of recipient mice. The hALB synthesis rate was approximately 23-times higher than that in liver tissue from transplanted HSs one week after transplantation (Fig. 6A). Although there was a minor decrease after transplantation, the VSLTs maintained higher hALB and hA1AT expression levels for 4 weeks (Fig. 6A, B). The transplantation of EHFS was more effective than the transplantation of co-suspension of hepatocytes and fibroblasts (Fig. 6C).

## 4. Discussion

Both types of hepatocyte sheets could be harvested at 4 days after the seeding of hepatocytes (Fig. 2B). Interestingly, EHFSs were more easily detached due to the forceful contraction of fibroblasts and formed thicker morphology (Fig. 2D, E). In addition, EHFSs could be harvested from TRCDs only one day after the seeding of hepatocytes onto fibroblast confluent (Supplementary Fig. 1A). The most rapid construction of EHFSs was achieved about 3 h after the inoculation of TIG-118 cells (Supplementary Fig. 1B). The TIG-118 cell layer could form on FBS-coated TRCD within 1 h when seeded at high cell density ( $1.56 \times 10^5$  cells/cm<sup>2</sup>), and EHFSs could be harvested soon after the adhesion of hepatocytes. These advantages of EHFS could aid in easy manipulation during transplantation and could be used for emergency such as acute liver failure. Similar advantages for rapid construction and sheet characteristics were described for our previously engineered HepaRC

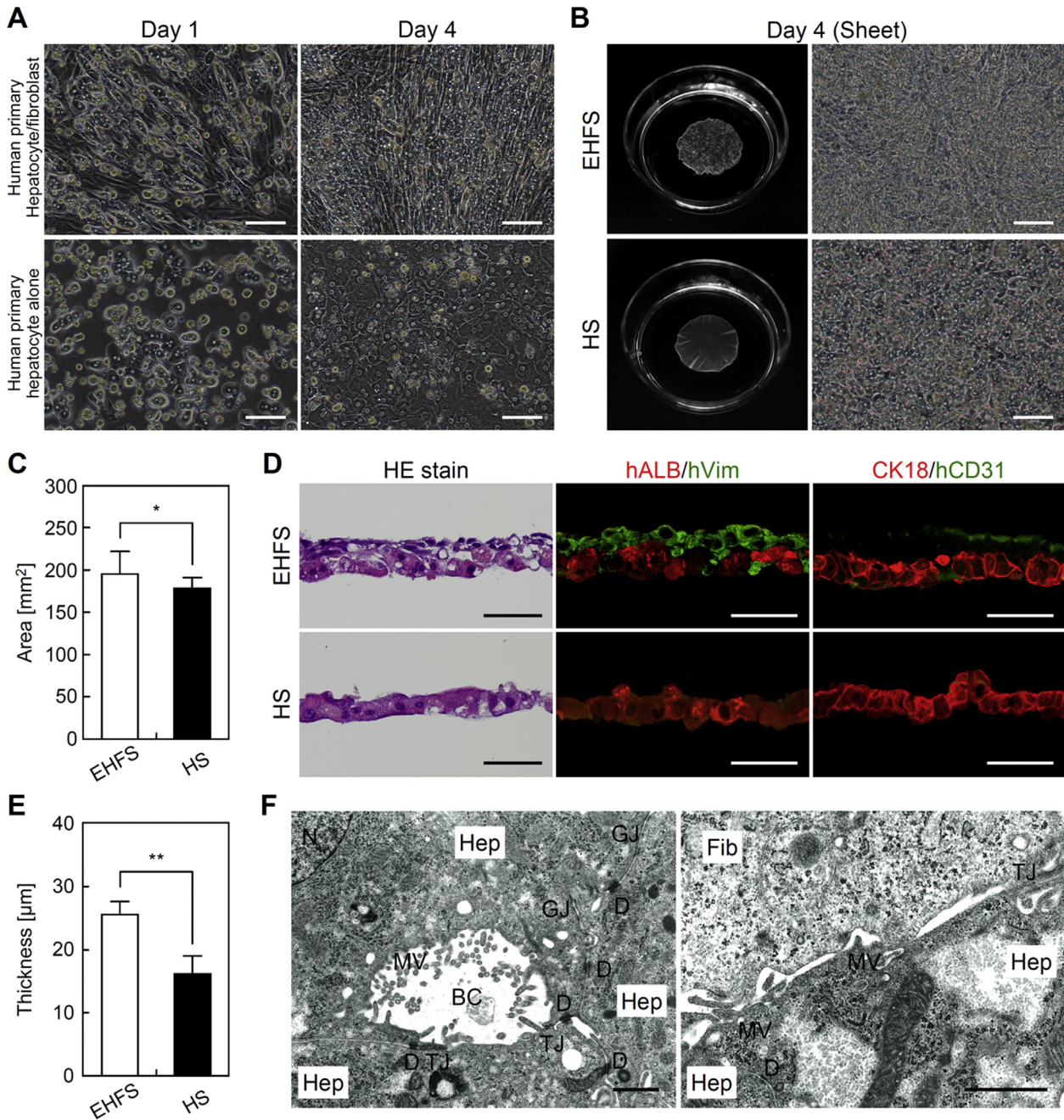


**Fig. 2.** Characterization of EHFSSs. (A) Phase-contrast micrographs of hepatocytes cultured on TRCDs. Above, human primary hepatocytes and fibroblasts; below, hepatocytes alone. Scale bar, 100  $\mu\text{m}$ . (B) Macroscopic and phase-contrast images of EHFSSs and HSs. Scale bar, 100  $\mu\text{m}$ . (C) Areas ( $n \geq 11$  from 2 independent preparations) of EHFSSs (open columns) and HSs (closed columns). Mean  $\pm$  SD, \* $P < 0.05$  (Welch's *t*-test). (D) HE and immunofluorescence staining of sheet cross-sections. Scale bar, 50  $\mu\text{m}$ . (E) Thicknesses ( $n \geq 9$  from 4 independent preparations) of EHFSSs (open columns) and HSs (closed columns). Mean  $\pm$  SD, \*\* $P < 0.01$  (Welch's *t*-test). (F) TEM images of EHFSS cross-sections. Scale bar, 1  $\mu\text{m}$ . Hep, hepatocyte; Fib, fibroblast; N, nucleus; MV, microvillus; BC, bile canal; TJ, tight junction; D, desmosome; GJ, gap junction; N.S., not significant.

cell/fibroblast sheets compared to HepaRG cell sheets from monoculture [27].

Subcutaneous transplantation of the EHFSSs would allow for minimally invasive hepatocyte-based therapy as well as possible retransplantation and removal of grafts if necessary [18,20–22]. However, graft failure occurs frequently [2,5,17,23]. The major reason for engraftment failure has been the insufficient number of blood vessels at the site of transplantation and the lack of vascular infiltration into the new tissue. To overcome this limitation, previous studies have induced subcutaneous vascularization by implanting a device for controlled release of acidic fibroblast

growth factor, bFGF, or VEGF, but it took at least 10 days for vascular bed formation [24,28,29]. Quite amazingly, grossly-visible VSLT, which had numerous blood vessels, were observed by day 7 after transplantation (Fig. 4D) without pre-transplant vascularization. This result will be caused by the continuous releasing of the angiogenic factors from the EHFSSs (Fig. 3B, C, E) instead of implanting a device for subcutaneous vascularization. Furthermore, the mRNA expressions (VEGF, TGF- $\beta$ 1, and HGF) of VSLTs from EHFSSs maintained at least 2 weeks after transplantation, and the expression levels compared favorably with those of EHFSSs (Supporting information and Supplementary Fig. 2).

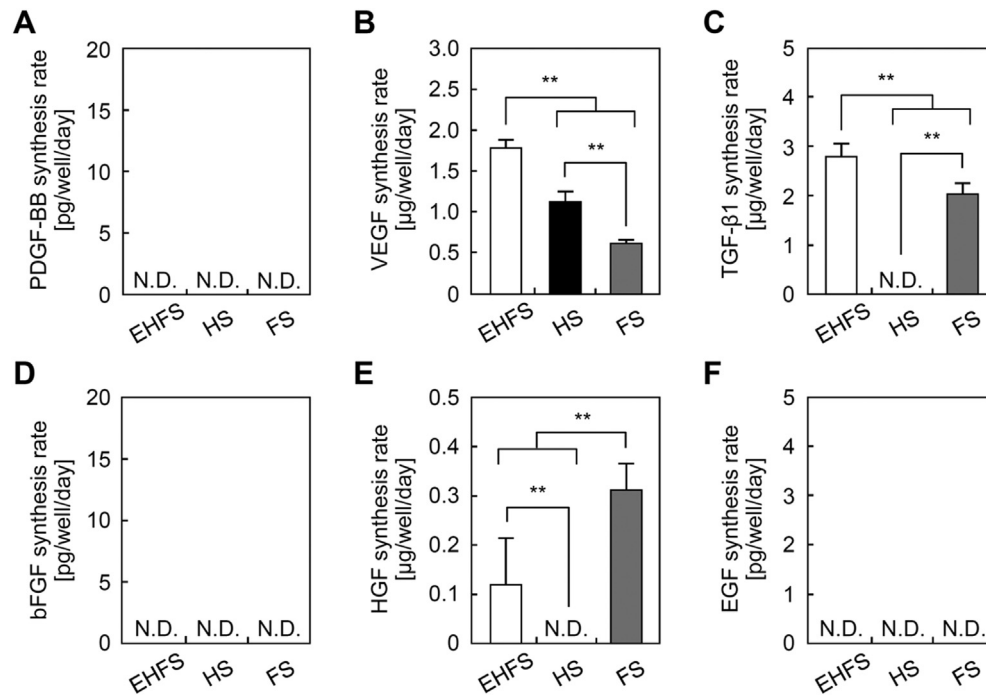


**Fig. 3.** *In vitro* synthesis rates of growth factors involved in angiogenesis. (A) Human PDGF-BB, (B) VEGF, (C) TGF-β1, (D) bFGF, (E) HGF, and (F) EGF ( $n \geq 17$  from 2 independent cell preparations). Open, closed, and shaded columns represent EHFSs, HSs, and FSs, respectively. Mean  $\pm$  SD,  $**p < 0.01$  (one-way ANOVA). N.D., not detected.

We show the model of VSLT construction in Fig. 7. The VSLTs were thick tissue comprising hepatocytes despite the low expression of Ki67 (Fig. 4A), which means that VSLT thickness resulted from the survival and self-aggregation of transplanted hepatocytes, followed by neoangiogenesis (Fig. 4B, C). The regulation of hepatocyte growth can be blamed on high TGF-β1 synthesis from fibroblasts (Fig. 3C) [30]. To improve the effect of subcutaneously transplanted hepatocytes, we should try to modify our system to allow the regulation of TGF-β1 synthesis. The aggregated hepatocytes in the outer end of VSLTs were hypertrophy at 7 days after transplantation because a temporary increasing of blood pressure will occur in the areas due to the discontinuity of blood vessels (Fig. 4A, D). The phenomenon was usually observed under high portal blood pressure condition after the partial hepatectomy [31]. Vascular network could perfuse blood when these discontinuous blood vessels connected with themselves; thus, the VSLTs indicated an increased red color (Fig. 4E). Hypertrophied hepatocytes were rarely observed at 14 days after transplantation (Fig. 4A) because the local blood pressure had decreased from vascular network formation. To reveal the origin of ECs, the immunochemical staining (non-specific species CD31 and human CD31) of VSLTs at 1, 7, and 14 days after EHFS transplantation were performed. As a result, almost all ECs at 7 days were from the host mice (non-specific species CD31-positive, hCD31-negative) (Fig. 4A). The number of CD31-positive cells at 14 days was higher than that at 7 days; thus, these vascular vessels grew into VSLTs from mice. However, hCD31-positive ECs could also be detected at 14 days. Very few human ECs in the cell suspension may proliferate during later period.

VSLTs showed high synthesis of liver-specific functions and reconstruction of structures (Fig. 5). At 2 weeks after EHFS transplantation, VSLTs consisted of several linearly located hepatocytes and abundant blood vessels, which were similar to hepatic lobule structures (Fig. 5A, B) [7]. In detail, hepatocytes are adjacent to microvessels through MVs, which is remarkably similar to the space of Disse (Fig. 5C). These structures permit VSLTs of 300-μm thickness to remain alive despite exceeding the limit of cell sheet

thickness for effective oxygen diffusion/supply (approximately 40 μm) [32–34]. Liver-specific ultrastructures, such as BCs, between hepatocytes were also reconstructed *in vivo*. These human hepatocytes expressed liver-specific functions *in vivo*, including hALB, hA1AT, and hF9 (Fig. 5B). In the future, VSLT could also assist in the development of several useful assays, such as novel systems to assess drug transport, and the treatment of hemophilia.

The human ALB and A1AT synthesis activities of VSLTs were exceedingly higher than those in the liver tissue derived from transplanted HSs (Fig. 6A, B). Takebe et al. [2] reported that the kidney subcapsule was a superior transplantation site compared with various ectopic sites, such as cranium and mesentery. However, they also showed that human adult hepatocytes ( $4.0 \times 10^6$  cells) transplanted under the kidney subcapsule of mouse could not keep producing high levels of hALB and showed a peak at day 15 (approximately 1200 ng/mL). Chen et al. [5] reported that their system for creating human ectopic artificial liver was ineffective for engraftment to the subcutaneous space. In contrast, VSLTs showed high levels of function despite the fact that VSLTs consisted of no more than  $1.0 \times 10^6$  subcutaneously implanted hepatocytes. At 4 weeks after transplantation, VSLTs maintained these functions (hALB,  $1132 \pm 553$  ng/mL; hA1AT,  $193 \pm 62$  ng/mL), although there were no significant differences. HE stained images of VSLT showed hepatocyte survival and support the high liver-specific protein syntheses (Supplementary Fig. 3A). On the other hand, the hepatocytes from HS were not readily apparent (Supplementary Fig. 3B). EHFS was more effective than co-suspension, as evidenced by results from well engraftment of the sheet format cell organoid (Fig. 6C). Almost all hepatocyte at 1 week after co-suspension transplantation were hypertrophic and formed thin tissue (Supplementary Fig. 3C). This fact highlighted the benefit of hepatocyte sheet such as enough extracellular matrix components and well-graft on site without wide spreading. However, we were concerned that exceedingly-high TGF-β1 synthesis of EHFS may trigger a part of hepatocytes to be apoptosis [31] and possibly-caused this minor decrease. Thus, this cell therapy has the

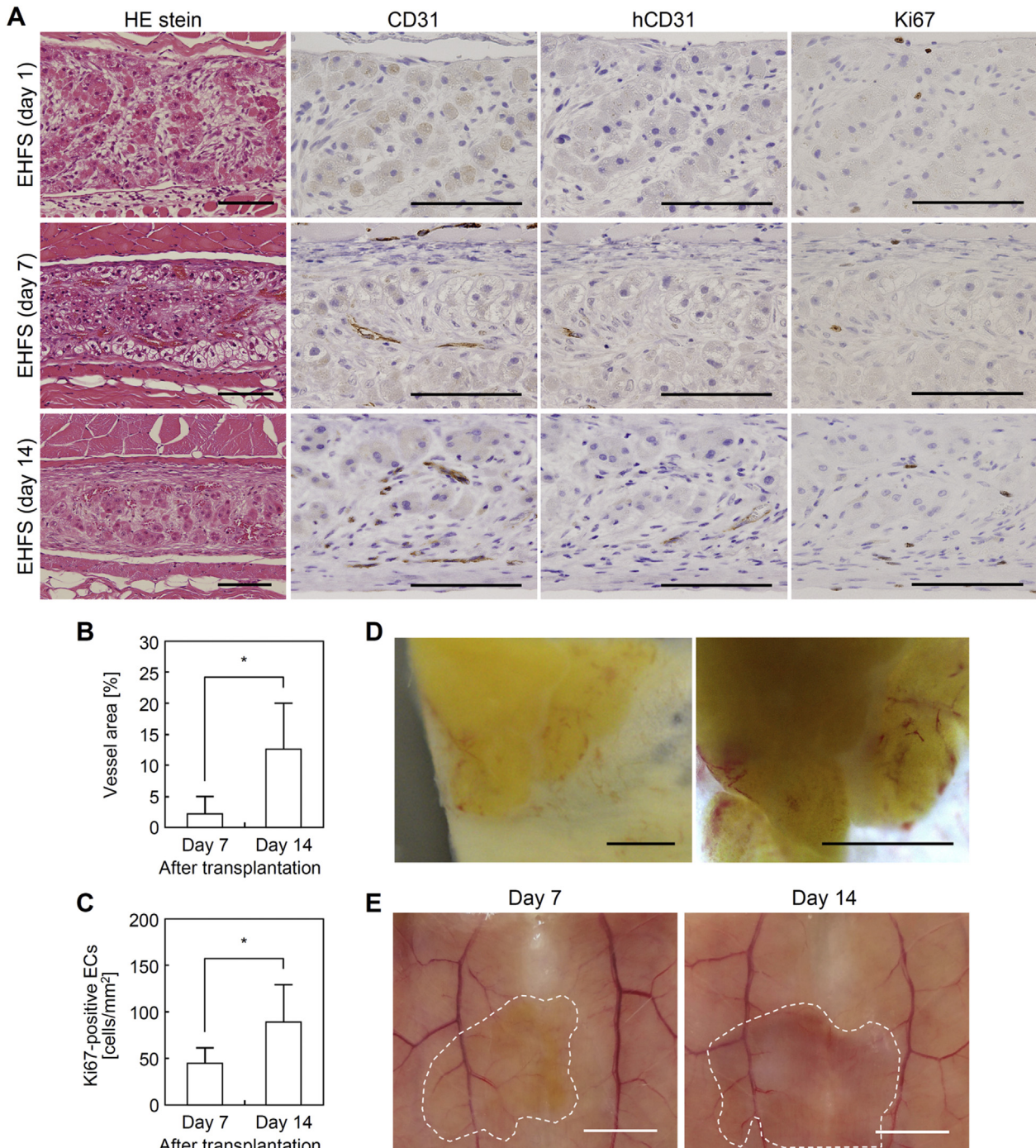


**Fig. 4.** Development of VSLTs *in vivo*. (A) Temporal HE and immunohistochemical staining of VSLT cross-sections at 1, 7, and 14 days after EHFS transplantation. Scale bar, 100  $\mu$ m. (B) Vessel area and (C) number of Ki67-positive ECs in VSLTs at 7 and 14 days after EHFS transplantation ( $n = 6$  from more than 4 independent cell preparations). Mean  $\pm$  SD, \* $P < 0.05$  (Welch's *t*-test). (D) Macroscopic image and phase-contrast micrograph of blood vessels in the VSLTs at 7 days after EHFS transplantation. Scale bar, 1 mm. (E) Macroscopic images of skin at 7 and 14 days after EHFS transplantation. Scale bar, 5 mm. The dashed lines indicate the VSLTs.

possibility of improvement in additional cell sources and/or medications for long-term cell therapy of chronic liver failure.

One of the most important differences from previous techniques is the safety of the cell sources. The use of mature hepatocytes and fibroblasts eliminates the risks of unanticipated differentiation fate, tumorigenic transformation [35–37], and tumor growth by mesenchymal stem cell accumulation at the tumor site [38,39]. Next, the VSLTs were constructed from easily cultured cells using simple procedures. This system employed normal human dermal

fibroblasts, which are easily cultured and proliferate rapidly, and requires no separate *in vitro* or *in vivo* vascularization methods before transplantation, such as mixing human umbilical vein endothelial cells with the cultured tissue and/or pre-implanting a bFGF-releasing device at the transplantation site. In addition, this system could allow for rapid large-scale production of transplantable tissue because it takes as little as 3 h for construction of EHFSs after seeding of fibroblasts. Such a system could be used in emergent circumstances associated with liver surgery, such as

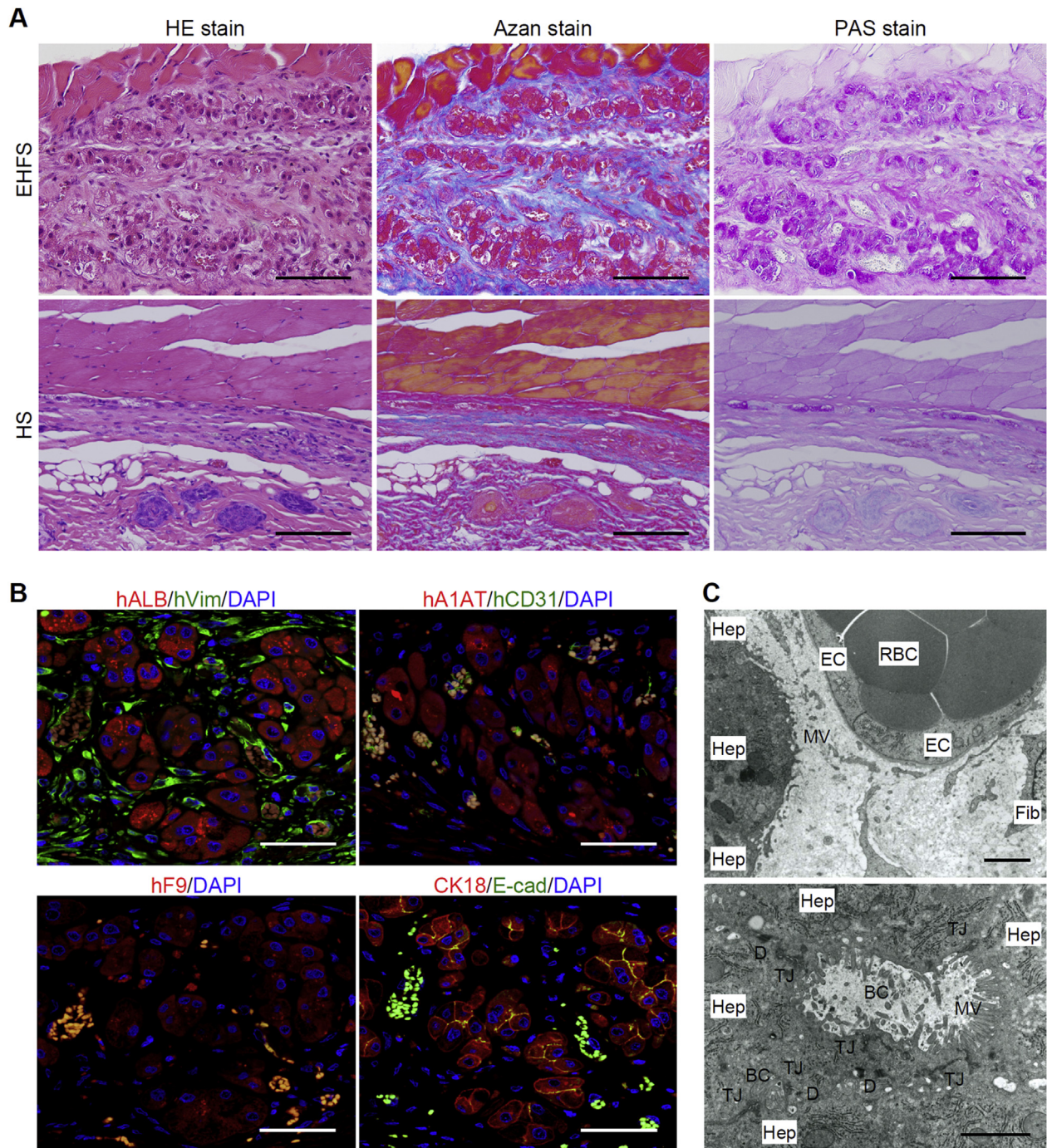


**Fig. 5.** Functional VSLTs under mouse skin at 2 weeks after transplantation. (A) HE, Azan, and PAS staining of VSLT cross-sections. Scale bar, 100 μm. (B) Immunofluorescence staining of VSLT cross-sections. Scale bar, 50 μm. (C) TEM images of VSLT cross-sections. Scale bar, 2 μm. Hep, hepatocyte; Fib, fibroblast; EC, endothelial cell; RBC, red blood cell, MV, microvillus; BC, bile canal; TJ, tight junction; D, desmosome.

autologous hepatocyte transplantation, because EHFSSs can be produced during the operation. This simple and rapid procedure is a major advance toward clinical application of subcutaneous liver tissue transplantation. Finally, more improvement of transplantation efficiency could require optimization of other cell sources, sheet forming process, combination of growth factors, and/or pre-transplant vascularization; thus, we will investigate these subjects as the next step for treatment liver diseases. Moreover, identical expression patterns of angiogenic factor syntheses *in vitro* and liver-specific functions *in vivo* were observed when HepaRG

cells were employed instead of human primary hepatocytes to create EHFSSs (Supplementary Fig. 4, 5). Thus, this versatile fibroblast system could be used for the construction of subcutaneous organs by using several functional cells such as islet of the pancreas.

## 5. Conclusion

We demonstrate viable VSLT derived from simple one-time subcutaneous transplantation of EHFSSs. This system, which



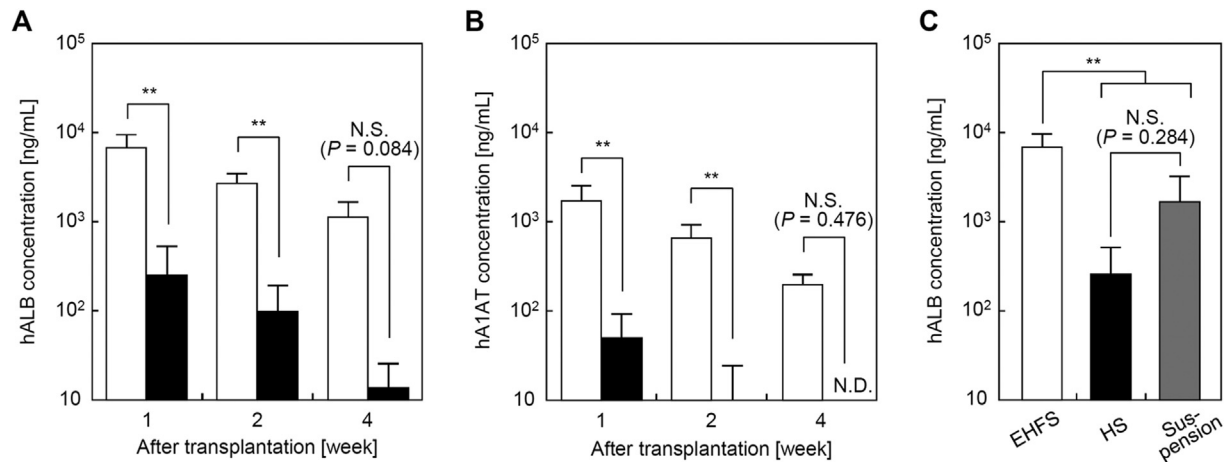


**Fig. 6.** *In vivo* liver-specific functions in mice. (A) hALB and (B) hA1AT concentrations in NOD SCID mouse serum ( $n \geq 10$  from 2 independent cell preparations). (C) hALB concentrations in NOD SCID mouse serum at 1 week after transplantation ( $n \geq 6$  from 2 independent preparations). Open, closed, and shaded columns represent EHFSs, HSs, and co-suspension of hepatocytes and fibroblasts, respectively. Mean  $\pm$  SD,  $**P < 0.01$  (two-way or one-way ANOVA). N.S., not significant; N.D., not detected.

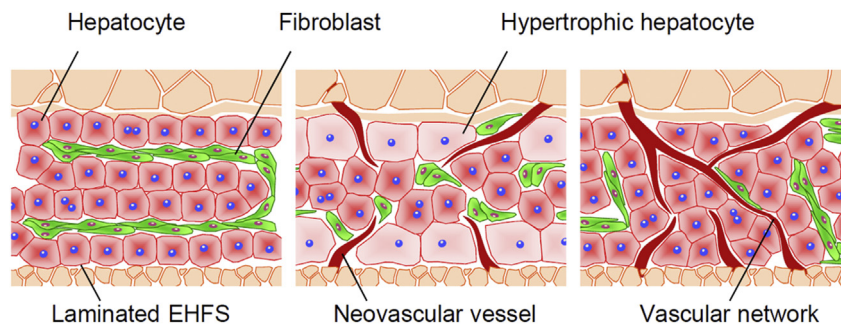


**Fig. 7.** Model of VSLT construction.

consists of cell sheet technology and co-culturing fibroblasts without pre-transplant procedures, was able to overcome the low transplantation efficiency of previous subcutaneous transplantation procedures. In addition, the transplant site and cell types employed could realize goals for the procedure to be minimally invasive and drastically safe. The resulting VSLTs could be used for the treatment of acute hepatic failure and inherited liver diseases. Furthermore, this system can be applied not only to hepatocytes but also to other cell types. Thus, our novel fibroblast system could be used to rapidly construct subcutaneous vascularized organs.

#### Source of funding

This work was supported in part by Grants-in-Aid for Young Scientists to Y. Sakai (no. 25861161) and Scientific Research to S. Eguchi (no. 23591868 and no. 26461916), Takeda Science Foundation to Y. Sakai, the Regenerative Medicine Support Project in Nagasaki Prefecture, and Creation of Innovation Centers for Advanced Interdisciplinary Research Areas Program in Project for Developing Innovation Systems, from the Ministry of Education, Culture, Sports, Science, and Technology (MEXT) of Japan to K. Ohashi.

#### Appendix A. Supplementary data

Supplementary data related to this article can be found at <http://dx.doi.org/10.1016/j.biomaterials.2015.06.046>.

#### References

- [1] T. Takebe, N. Koike, K. Sekine, R. Fujiwara, T. Amiya, Y.W. Zheng, et al., Engineering of human hepatic tissue with functional vascular networks, *Organogenesis* 10 (2014) 260–267.
- [2] T. Takebe, K. Sekine, M. Enomura, H. Koike, M. Kimura, T. Ogaeri, et al., Vascularized and functional human liver from an iPSC-derived organ bud transplant, *Nature* 499 (2013) 481–484.
- [3] H. Sekine, T. Shimizu, K. Sakaguchi, I. Dobashi, M. Wada, M. Yamato, et al., In vitro fabrication of functional three-dimensional tissues with perfusable blood vessels, *Nat. Commun.* 4 (2013) 1399.
- [4] J.S. Miller, K.R. Stevens, M.T. Yang, B.M. Baker, D.H. Nguyen, D.M. Cohen, et al., Rapid casting of patterned vascular networks for perfusable engineered three-dimensional tissues, *Nat. Mater.* 11 (2012) 768–774.
- [5] A.A. Chen, D.K. Thomas, L.L. Ong, R.E. Schwartz, T.R. Golub, S.N. Bhatia, Humanized mice with ectopic artificial liver tissues, *Proc. Natl. Acad. Sci. U. S. A.* 108 (2011) 11842–11847.
- [6] T. Sasagawa, T. Shimizu, S. Sekiya, Y. Haraguchi, M. Yamato, Y. Sawa, et al., Design of prevascularized three-dimensional cell-dense tissues using a cell sheet stacking manipulation technology, *Biomaterials* 31 (2010) 1646–1654.
- [7] S.N. Bhatia, U.J. Balis, M.L. Yarmush, M. Toner, Effect of cell-cell interactions in preservation of cellular phenotype: cocultivation of hepatocytes and non-parenchymal cells, *FASEB J.* 13 (1999) 1883–1900.
- [8] K. Kim, K. Ohashi, R. Utoh, K. Kano, T. Okano, Preserved liver-specific functions of hepatocytes in 3D co-culture with endothelial cell sheets, *Biomaterials* 33 (2012) 1406–1413.
- [9] Y. Sakai, S. Yamagami, K. Nakazawa, Comparative analysis of gene expression in rat liver tissue and monolayer- and spheroid-cultured hepatocytes, *Cells Tissues Organs* 191 (2010) 281–288.
- [10] R.J. Thomas, R. Bhandari, D.A. Barrett, A.J. Bennett, J.R. Fry, D. Powe, et al., The effect of three-dimensional co-culture of hepatocytes and hepatic stellate cells on key hepatocyte functions in vitro, *Cells Tissues Organs* 181 (2005) 67–79.
- [11] S.F. Abu-Abisi, J.R. Friend, L.K. Hansen, W.S. Hu, Structural polarity and functional bile canaliculi in rat hepatocyte spheroids, *Exp. Cell Res.* 274 (2002) 56–67.
- [12] N. Koide, K. Sakaguchi, Y. Koide, K. Asano, M. Kawaguchi, H. Matsushima, et al.

- al., Formation of multicellular spheroids composed of adult rat hepatocytes in dishes with positively charged surfaces and under other nonadherent environments, *Exp. Cell Res.* 186 (1990) 227–235.
- [13] J. Kasuya, R. Sudo, T. Mitaka, M. Ikeda, K. Tanishita, Spatio-temporal control of hepatic stellate cell-endothelial cell interactions for reconstruction of liver sinusoids in vitro, *Tissue Eng. Part A* 18 (2012) 1045–1056.
- [14] F. Evenou, T. Fujii, Y. Sakai, Spontaneous formation of highly functional three-dimensional multilayer from human hepatoma Hep G2 cells cultured on an oxygen-permeable polydimethylsiloxane membrane, *Tissue Eng. Part C Methods* 16 (2010) 311–318.
- [15] R.D. Guarino, L.E. Dike, T.A. Haq, J.A. Rowley, J.B. Pitner, M.R. Timmins, Method for determining oxygen consumption rates of static cultures from microprobe measurements of pericellular dissolved oxygen concentration, *Biotechnol. Bioeng.* 86 (2004) 775–787.
- [16] B.E. Uygun, A. Soto-Gutierrez, H. Yagi, M.L. Izamis, M.A. Guzzardi, C. Shulman, et al., Organ reengineering through development of a transplantable recellularized liver graft using decellularized liver matrix, *Nat. Med.* 16 (2010) 814–820.
- [17] H. Lee, R.A. Cusick, H. Utsunomiya, P.X. Ma, R. Langer, J.P. Vacanti, Effect of implantation site on hepatocytes heterotopically transplanted on biodegradable polymer scaffolds, *Tissue Eng.* 9 (2003) 1227–1232.
- [18] K. Ohashi, F. Park, M.A. Kay, Hepatocyte transplantation: clinical and experimental application, *J. Mol. Med.* 79 (2001) 617–630.
- [19] C.B. Kemp, M.J. Knight, D.W. Scharp, W.F. Ballinger, P.E. Lacy, Effect of transplantation site on the results of pancreatic islet isografts in diabetic rats, *Diabetologia* 9 (1973) 486–491.
- [20] K. Ohashi, Liver tissue engineering: the future of liver therapeutics, *Hepatol. Res.* 38 (2008) S76–87.
- [21] I.J. Fox, D.F. Schafer, G.R. Yannam, Finding a home for cell transplants: location, location, location, *Am. J. Transpl. Med.* 6 (2006) 5–6.
- [22] A. Pileggi, R.D. Molano, C. Ricordi, E. Zahr, J. Collins, R. Valdes, L. Inverardi, Reversal of diabetes by pancreatic islet transplantation into a subcutaneous, neovascularized device, *Transplantation* 81 (2006) 1318–1324.
- [23] S.W. Lee, X. Wang, N.R. Chowdhury, J. Roy-Chowdhury, Hepatocyte transplantation: state of the art and strategies for overcoming existing hurdles, *Ann. Hepatol.* 3 (2004) 48–53.
- [24] K. Ohashi, T. Yokoyama, M. Yamato, H. Kuge, H. Kanehiro, M. Tsutsumi, et al., Engineering functional two- and three-dimensional liver systems in vivo using hepatic tissue sheets, *Nat. Med.* 13 (2007) 880–885.
- [25] S.C. Strom, R.L. Jirtle, R.S. Jones, D.L. Novicki, M.R. Rosenberg, A. Novotny, et al., Isolation, culture, and transplantation of human hepatocytes, *J. Natl. Cancer Inst.* 68 (1982) 771–778.
- [26] P.O. Seglen, Preparation of isolated rat liver cells, *Methods Cell Biol.* 13 (1976) 29–83.
- [27] Y. Sakai, M. Koike, H. Hasegawa, K. Yamanouchi, A. Soyama, M. Takatsuki, et al., Rapid fabricating technique for multi-layered human hepatic cell sheets by forceful contraction of the fibroblast monolayer, *PLoS One* 8 (2013) e70970.
- [28] M.K. Smith, K.W. Riddle, D.J. Mooney, Delivery of hepatotrophic factors fails to enhance longer-term survival of subcutaneously transplanted hepatocytes, *Tissue Eng.* 12 (2006) 235–244.
- [29] T. Yokoyama, K. Ohashi, H. Kuge, H. Kanehiro, H. Iwata, M. Yamato, et al., In vivo engineering of metabolically active hepatic tissues in a neovascularized subcutaneous cavity, *Am. J. Transpl. Med.* 6 (2006) 50–59.
- [30] T. Ichikawa, Y.Q. Zhang, K. Kogure, Y. Hasegawa, H. Takagi, M. Mori, et al., Transforming growth factor beta and activin tonically inhibit DNA synthesis in the rat liver, *Hepatology* 34 (2001) 918–925.
- [31] Y. Miyaoka, K. Ebato, H. Kato, S. Arakawa, S. Shimizu, A. Miyajima, Hypertrophy and unconventional cell division of hepatocytes underlie liver regeneration, *Curr. Biol.* 22 (2012) 1166–1175.
- [32] W. Sekine, Y. Haraguchi, T. Shimizu, A. Umezawa, T. Okano, Thickness limitation and cell viability of multi-layered cell sheets and overcoming the diffusion limit by a porous-membrane culture insert, *J. Biochip Tissue chip* (2011), <http://dx.doi.org/10.4172/2153-0777.S1-007>.
- [33] Y. Sakai, K. Nakazawa, Technique for the control of spheroid diameter using microfabricated chips, *Acta Biomater.* 3 (2007) 1033–1040.
- [34] J. Fukuda, K. Okamura, K. Nakazawa, H. Ijima, Y. Yamashita, M. Shimada, et al., Efficacy of a polyurethane foam/spheroid artificial liver by using human hepatoblastoma cell line (Hep G2), *Cell Transpl.* 12 (2003) 51–58.
- [35] K. Okita, M. Nakagawa, H. Hyenjong, T. Ichisaka, S. Yamanaka, Generation of mouse induced pluripotent stem cells without viral vectors, *Science* 322 (2008) 949–953.
- [36] H. Hentze, R. Graichen, A. Colman, Cell therapy and the safety of embryonic stem cell-derived grafts, *Trends Biotechnol.* 25 (2007) 24–31.
- [37] J. Yu, M.A. Vodyanik, K. Smuga-Otto, J. Antosiewicz-Bourget, J.L. Frane, S. Tian, et al., Induced pluripotent stem cell lines derived from human somatic cells, *Science* 318 (2007) 1917–1920.
- [38] R. Uchibori, T. Tsukahara, H. Mizuguchi, Y. Saga, M. Urabe, H. Mizukami, et al., NF- $\kappa$ B activity regulates mesenchymal stem cell accumulation at tumor sites, *Cancer Res.* 73 (2013) 364–372.
- [39] M. Studeny, F.C. Marini, J.L. Dembinski, C. Zompetta, M. Cabreira-Hansen, B.N. Bekele, et al., Mesenchymal stem cells: potential precursors for tumor stroma and targeted-delivery vehicles for anticancer agents, *J. Natl. Cancer Inst.* 96 (2004) 1593–1603.